ELSEVIER

International Journal of Heat and Fluid Flow 20 (1999) 280–289

International Journal of HEAT AND FLUID FLOW

www.elsevier.com/locate/ijhff

Surface heat transfer and flow structures of steady and fully pulsed radial reattaching jets

K. Bremhorst *, N.D. Agnew

Department of Mechanical Engineering, The University of Queensland, Brisbane, QLD 4072, Australia

Abstract

Radial jet reattachment occurs when a radial jet positioned near a surface attaches to it. This results in higher surface heat transfer rates than with in-line jets impinging normal to the surface. Flow pulsing was used in an attempt to increase heat transfer but measurements showed no improvement over the steady case. Velocity measurements near the surface show that pulsing reduces the wall velocity gradient and Reynolds shear stresses relative to the exit jet momentum were also found to be lower than for the steady case. Computations with the basic k-ϵ model failed to predict a secondary flow in the recirculation region and gave only limited success in the prediction of pressure coefficients and Nusselt numbers.

Notation

b	nozzle slot width
D	in-line jet exit diameter
f	frequency of pulsation
H	distance of in-line jet from surface
k	turbulent kinetic energy $= \frac{1}{2}\overline{u_i u_i}$
M_s, M_p	steady jet momentum, pulsed jet momentum
N	on:off ratio for pulsed flow
Nu	Nusselt number
P	static pressure
Pr	Prandtl number
r	radial direction
r_0	radial distance to nozzle exit plane
T	fluid temperature
U	mean axial velocity (positive direction is from nozzle to surface)
U_τ	phase averaged mean axial velocity
u	velocity fluctuation
u_I	axial intrinsic velocity fluctuation
u'_I	root mean square intrinsic velocity, phase or pulse averaged
$\overline{uv}_I$	intrinsic covariance, phase or pulse averaged
V, V_τ, v'_I	as for U, U_τ and u'_I but in radial direction
V_0	nozzle exit velocity
x	axial coordinate
X_p	distance between nozzle and surface

1. Introduction

Many drying processes use jet impingement for transport of heat and mass in order to speed the process. Examples can be found in the paper industry where the wet sheet is dried as it passes between rollers of the production process. One method is to use in-line jets which direct a jet of hot air normal to the paper. A more recent innovation which has already found industry acceptance uses radial jet reattachment flow in order to increase transfer rates, Page and Kiel (1990). While surface heat transfer characteristics are well documented, Page and Kiel (1990), Ostawari and Page (1992), the flow processes are not well understood and no satisfactory modelling of such flows has been published.

Radial jet reattachment (RJR) flow is obtained when a radial jet operates sufficiently near a surface so that the entrainment by the jet causes it to deflect and attach to the surface. This results in a flow similar to that of a backward facing step except that the equivalent of a backward facing wall does not exist and more importantly perhaps, the flow is axisymmetric and diverging between the nozzle and the surface. The resultant jet leads to a reattachment circle where the stagnation streamline meets the surface. A cross-section of such a flow with the coordinate system to be used, is shown in Fig. 1.

Further improvements in heat transfer are being sought. Pepper (1993), adapted the whistler nozzle, Hill and Greene (1977), to the in-line jet in order to obtain unsteady flow as it is known from the earlier work, Crowe and Champagne (1971), that introduction of flow unsteadiness, leads to an increase in entrainment. Fully pulsed jet flow, Bremhorst and Hollis (1990), is also known to give significant increases in entrainment, although consistent with Taylor's entrainment hypothesis, it is found that the increase in entrainment is directly proportional to the jet's momentum, Bremhorst and Hollis (1990).

Flow visualization of the steady RJR nozzle flow, Agnew (1991), showed that the reattachment circle is not steady or

* Corresponding author. Tel.: +61 7 3365 3597; fax: +61 7 3365 4799; e-mail: bremhorst@mech.uq.edu.au.

0142-727X/99/$ – see front matter
PII: S0142-727X(99)00013-2

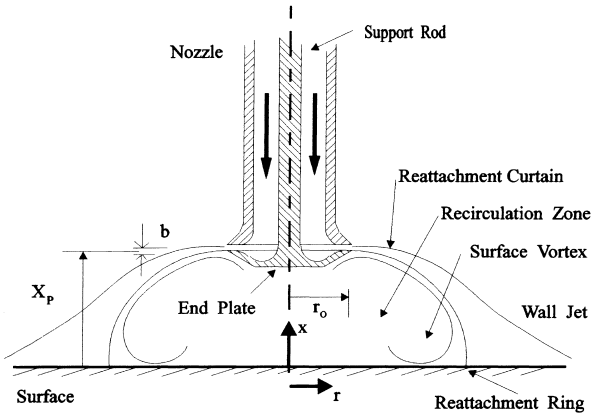

Fig. 1. Radial jet reattachment and coordinate system, $r_0 = 21.7$ mm.

closed at all times. Instead, it consists of periodic blowouts at random locations around the reattachment zone. This is distinctly different from the stagnation point of an in-line jet and was thought to be a contributing feature of the higher surface heat transfer experienced with RJR flow. Due to the trapped fluid within the reattachment curtain, a small area under the nozzle has low heat transfer rates. If fluid in that area can be removed periodically, a further increase in heat transfer was thought to be possible.

It was postulated that by use of a fully pulsed RJR flow which leads to periodic destruction of the reattachment curtain and its renewal, it should be possible to obtain considerable gains due to the increased temperature gradients at the wall with every cycle of fluid renewal.

The purpose of this paper is to report experimental results of investigations into steady and fully pulsed RJR flow produced by pulsing the mass flow to the radial jet nozzle in order to yield a periodically reattaching flow. Results of simple modelling of the steady case are presented together with an examination of the velocity field.

2. Experimental equipment

A crucial aspect of any jet flow studies is the initial condition of the jet as determined by the nozzle details. For the results reported here, a nozzle with an internally shaped flow path as shown in Fig. 1 was used, Agnew (1996). Hot-wire anemometer measurements at the exit of the nozzle verified that a near ideal top hat profile existed. The exit root mean square turbulence level was less than 7% of the mean exit velocity even for the largest exit gap.

Air was supplied from a compressed air source through filters to a plenum chamber. At the outlet of the plenum chamber, a rotating valve consisting of two geared counter-rotating rollers allowed full pulsing of the flow. A variable speed motor connected to the rollers was used to control the frequency of pulsation. Different sets of rollers gave different on:off ratios. A timing signal was generated by use of a fixed light beam and slotted disc attached to the roller When the rollers were fully open and not rotating, a smooth flow passage existed resulting in the steady RJR flow. The exit velocity time history for pulsed operation approximated a half sinusoid squared.

Flow rate was measured with a sonic nozzle thus preventing pressure fluctuations from the pulsing valve propagating upstream and affecting flow rate readings, Agnew (1996). In the

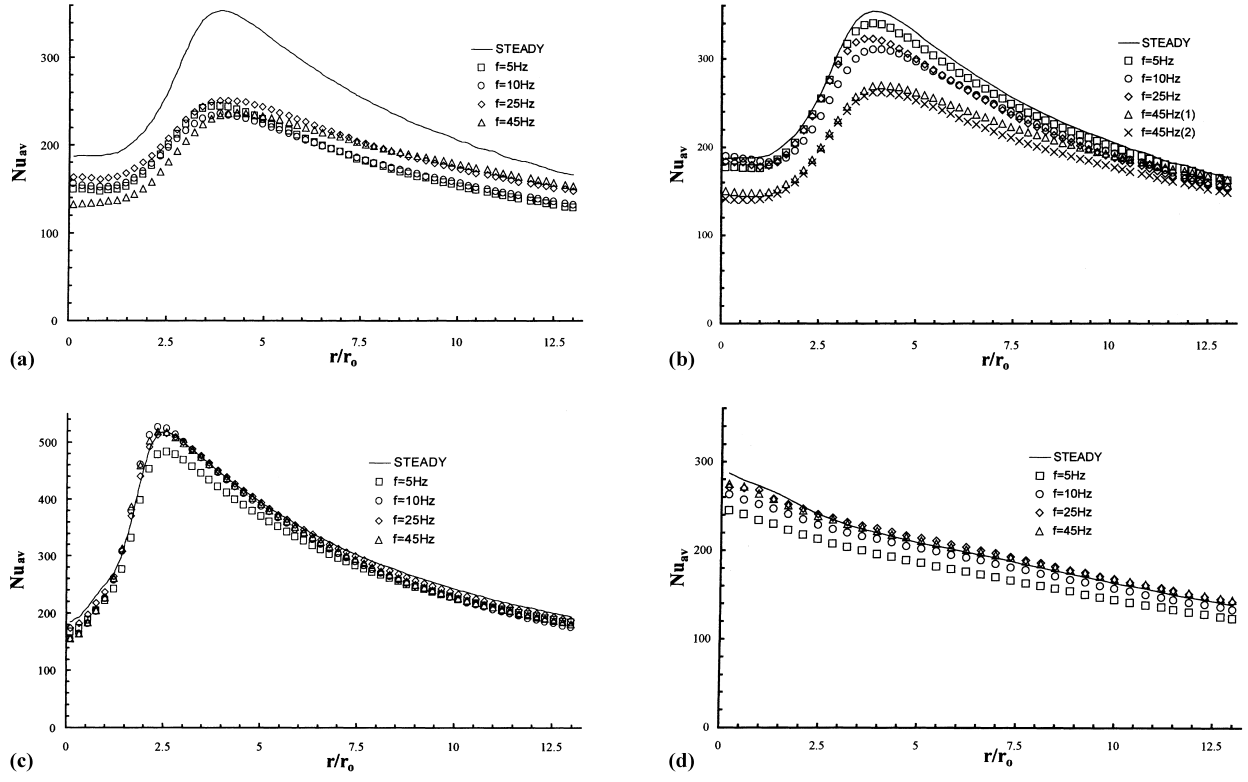

Fig. 2. (a) Average Nusselt number with RJR ($b = 2.5$ mm, $X_p = 24$ mm, $V_0 = 48$ m/s, $N = 1/3$). (b) Average Nusselt number with RJR ($b = 2.5$ mm, $X_p = 24$ mm, $V_0 = 48$ m/s, $N = 2/3$). (c) Average Nusselt number with RJR ($b = 2.5$ mm, $X_p = 10$ mm, $V_0 = 48$ m/s, $N = 2/3$). (d) Average Nusselt number with in-line nozzle ($H = 6$D, $V_0 = 48$ m/s, $N = 2/3$).

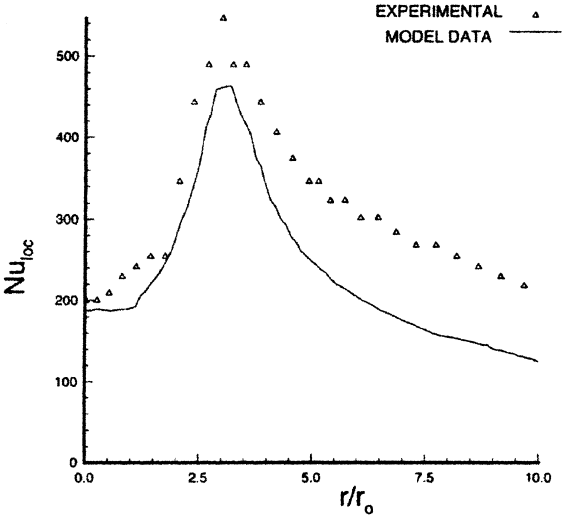

Fig. 3. Comparison of predicted and experimental local Nusselt numbers for steady RJR flow.

case of laser Doppler anemometer measurements, a venturi injector nozzle introduced seed particles into the air supply just upstream of the plenum chamber. The latter was sized to maintain pressure fluctuations during a pulsing cycle at or below 3% of the mean pressure.

Surface heat transfer measurements were performed on a heated INCONEL 600 sheet of 0.0254 mm thickness held on to a perspex table by a vacuum. This construction minimized heat losses. The foil was heated with a 50 A, 5 V dc power supply.

Local heat transfer coefficients were obtained from

$$h_{\mathrm{loc}} = \frac{(q''_{\mathrm{gen}} - q''_{\mathrm{rad}} - q''_{\mathrm{con}})}{(T_{\mathrm{h}} - T_{\mathrm{ad}})},$$

where T_{h} is the surface temperature when the foil is heated and T_{ad} is the adiabatic surface temperature. The foil surface was painted matte black to ensure ideal black body radiation. Both temperatures were measured with a MIKRON 6T62 infrared thermographic system with a maximum temperature resolution of 0.025°C giving an accuracy of better than ±0.5% over its operating range. The heat fluxes, q'', represent generation of heat within the foil, radiant loss of heat from the surface of the foil and heat loss from the foil by conduction to its support

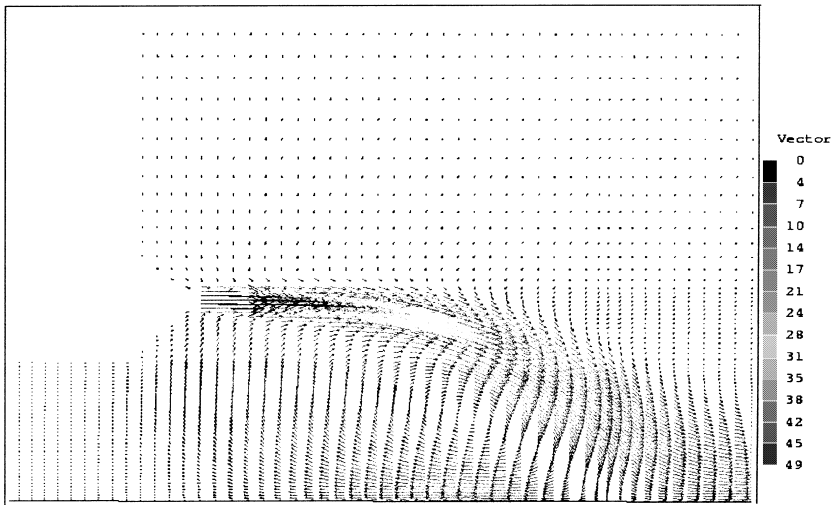

Fig. 4. Predicted velocity field of steady RJR flow.

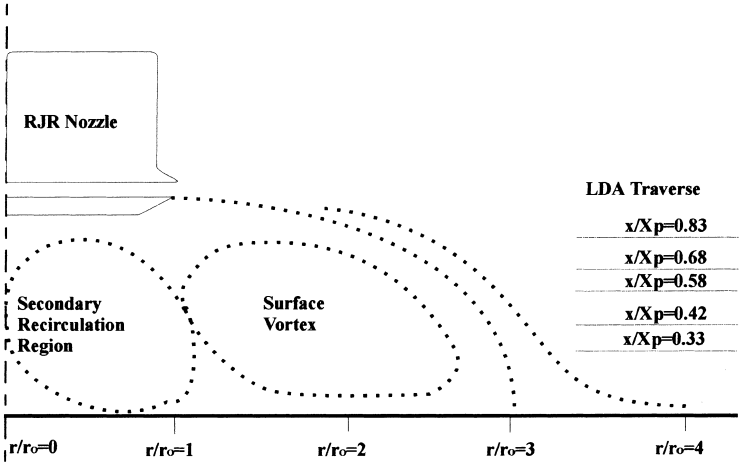

Fig. 5. Flow field deduced from U and V measurements – steady and pulsed flows are similar.

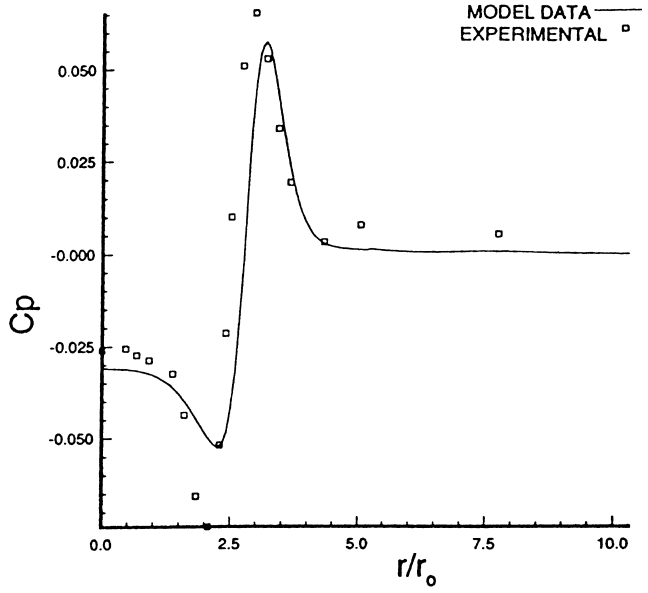

Fig. 6. Pressure coefficient distribution at surface for steady RJR flow ($b = 2.5$ mm, $X_p = 24$ mm, $V_0 = 48$ m/s).

base, respectively. From the local heat transfer coefficient values, area averages could be obtained to any radius.

Velocity field measurements were conducted with a TSI 3-beam argon–ion laser Doppler anemometer system with polarisation to achieve separation of channels. A 40 MHz Bragg cell was used for frequency shifting to maintain an adequate number of fringe crossings to avoid fringe bias during the high velocity section of the pulse.

Signal processing was by means of two TSI 1990A counter type processors interfaced with an IBM compatible PC. Sample-hold processing was employed to remove velocity bias while Doppler burst validation was performed with a 1% accuracy for 1:2 time comparisons. Sample rates to ensure minimal velocity bias were selected according to the following criterion, Winter et al. (1991).

$$\dot{N}T_u > 5$$

where $\dot{N}$ is the data rate and T_u is the integral time scale of the flow.

3. Surface heat transfer

Local Nusselt numbers, Bremhorst and Agnew (1996), for the RJR case can be integrated to yield the area averaged Nusselt numbers shown in Fig. 2(a)–(c). The smaller on:off ratio is seen to give the least favorable result irrespective of the size of surface over which the averages are formed. Some degree of pulsing frequency dependency is evidenced in all cases.

From the two results at $N = 2/3$, it is seen that the steady jet result was approached for the closer spacing between nozzle

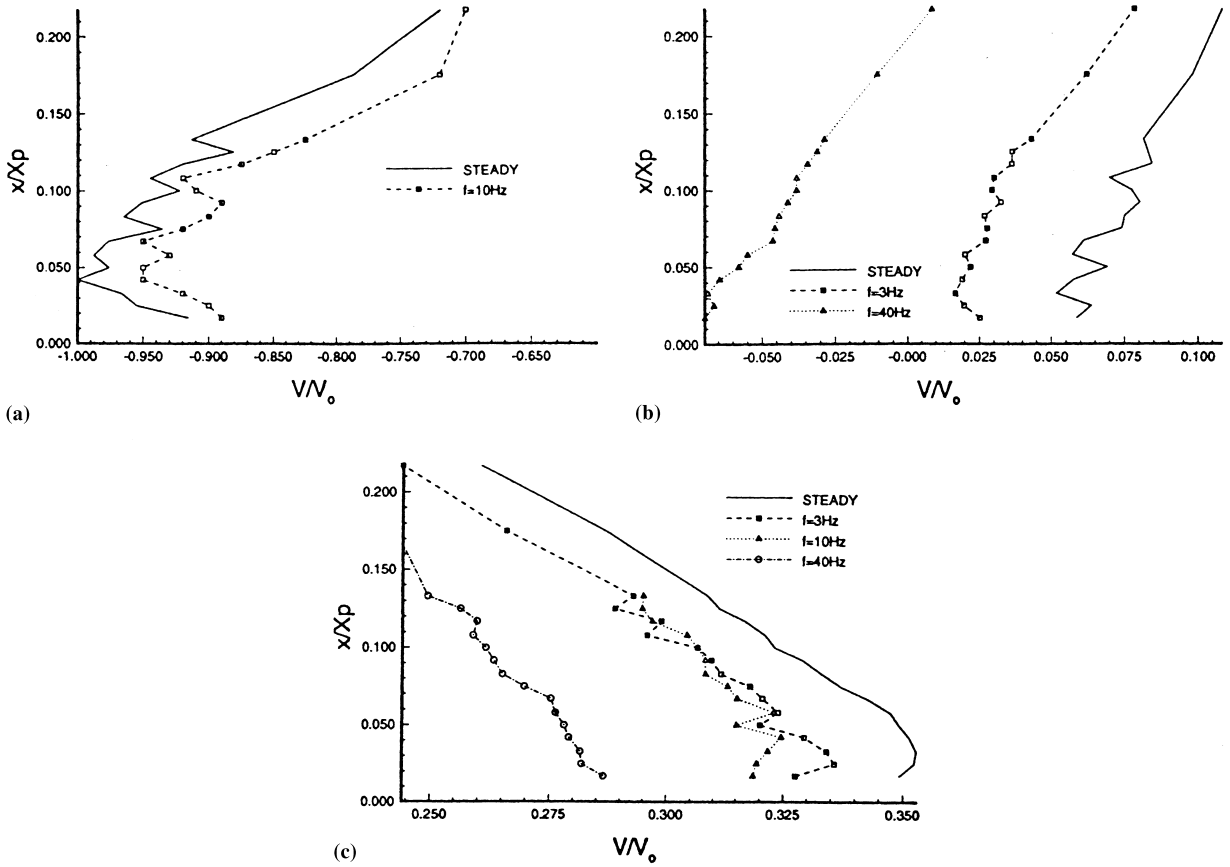

Fig. 7. (a) Mean radial velocity: $V_0 = 48$ m/s, $b = 2.5$ mm, $X_p = 24$ mm, $r/r_0 = 2$. (b) Mean radial velocity: $V_0 = 48$ m/s, $b = 2.5$ mm, $X_p = 24$ mm, $r/r_0 = 3.14$. (c) Mean radial velocity: $V_0 = 48$ m/s, $b = 2.5$ mm, $X_p = 24$ mm, $r/r_0 = 4.8$.

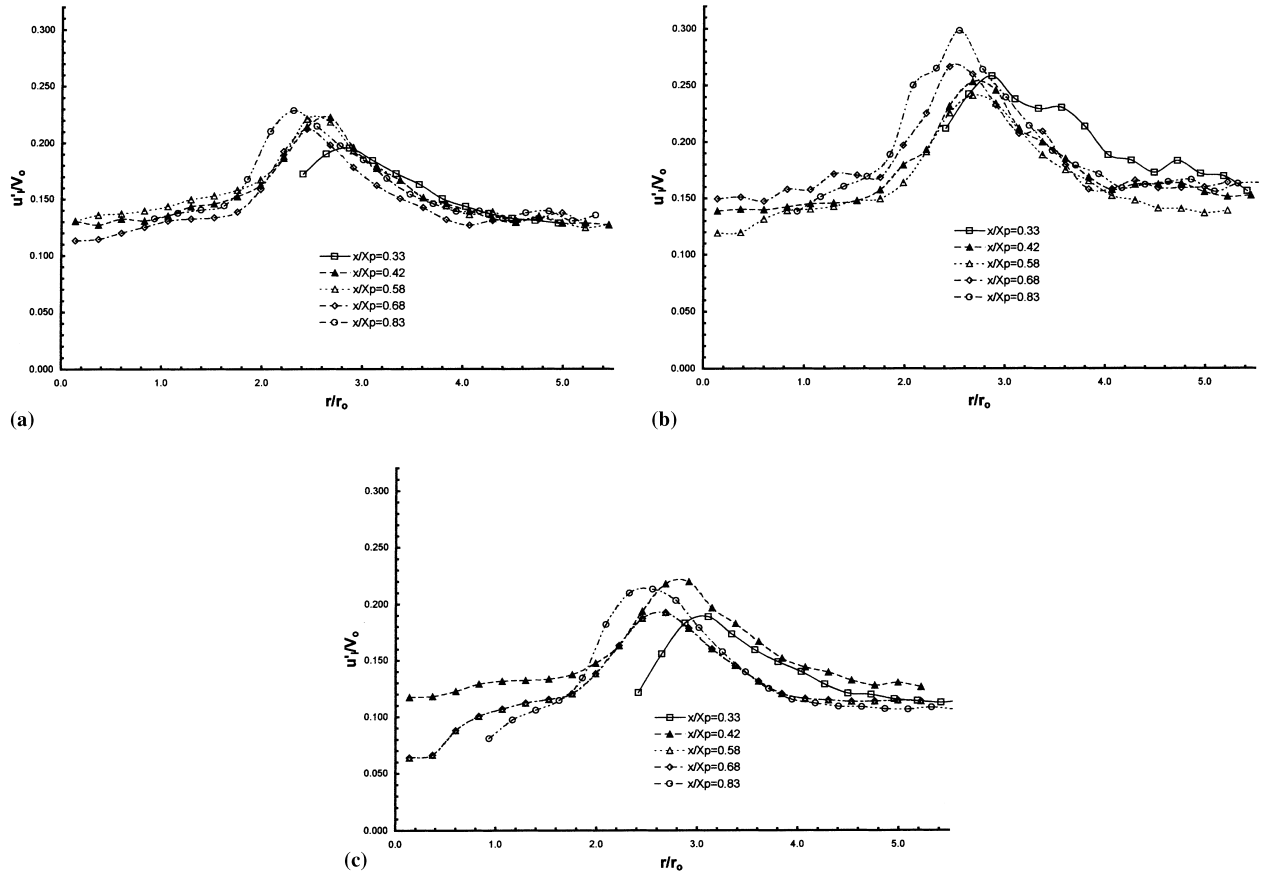

Fig. 8. (a) Intrinsic turbulence intensities for steady RJR flow: $V_0 = 48$ m/s, $b = 2.5$ mm, $X_p = 24$ mm. (b) Intrinsic turbulence intensities for pulsed RJR flow: $V_0 = 48$ m/s, $b = 2.5$ mm, $X_p = 24$ mm, 10 Hz pulsation frequency and $N = 1/3$. (c) Intrinsic turbulence intensities for pulsed RJR flow: $V_0 = 48$ m/s, $b = 2.5$ mm, $X_p = 24$ mm, 10 Hz pulsation frequency and $N = 2/3$.

and surface. None of the three cases led to average Nusselt numbers higher than the steady case although, for the case of Fig. 2(b), indications are that if lower frequencies of pulsation had been possible, the steady case may be exceeded. Due to the low thermal inertia of the thin heating foil, lower frequencies could not be tested as the surface temperature fluctuates with the pulsations. The larger frequency dependency for this case is probably due to the time taken to establish a reattachment curtain and the vortex flows within it. The increase in Nusselt number with decreasing distance between nozzle and surface suggests that further increases may be possible by bringing the nozzle still closer to the surface.

The effect of a one pixel shift of surface temperature readings with the imaging equipment is shown in Fig. 2(a) at the lowest frequency where some fluctuation of surface temperature was already evident. Repeatability of readings is demonstrated by the repeat result for 45 Hz in Fig. 2(b). Neither effect is seen to be significant in the final result.

Measurements were also taken with an in-line nozzle without the radially reattaching feature, Fig. 2(d). Pulsing is seen to make little difference to the average Nusselt number relative to the steady case but levels are well below those of the RJR flow.

Although only low subsonic flow existed, measured adiabatic surface temperatures varied across the surface for any given jet setting. This demonstrates the sensitivity of the thermal imaging equipment as well as the lack of radial conduction in the thin foil which forms the heat transfer surface.

4. Simulation of steady RJR flow

Notwithstanding the well documented shortcomings of the simple k-ϵ model for separated and impinging flows, an attempt was made to model one of the above RJR flows. The relevant equations are shown in Appendix A where $C_\mu = 0.09$, $C_{1\varepsilon} = 1.44$, $C_{2\varepsilon} = 1.92$, $\sigma_k = 1.0$ and $\sigma_\varepsilon = 1.3$. A turbulent Prandtl number, σ_T, of 0.86 was used to relate the eddy viscosity, ν_t , and eddy diffusivity.

In order to obtain a reattachment zone which is independent of the size of the computational domain, the flow field was solved to $r/r_0 = 10$ in the radial direction and to $x/r_0 = 7$ in the axial direction. Zero gradient boundary conditions were used along the open boundaries together with the no-slip condition at the wall. A wall function was included at the surface in order to speed up calculations using PHOENICS Ver. 2.0.

The predicted heat transfer result is shown in Fig. 3 and is compared with experimental data. Remarkably good agreement is noted for the location of the peak which corresponds to the reattachment line. For part of the region underneath the nozzle and the recirculation zone, predictions match measurements quite well but the region further downstream in the wall jet region as well as the level of the peak show significant disagreement between experiment and prediction.

Rather than extend computations to the pulsed case with the same model, a more detailed investigation of the flow field is presented to discover where shortcomings of the modelled results may exist for the steady case and to also obtain a better

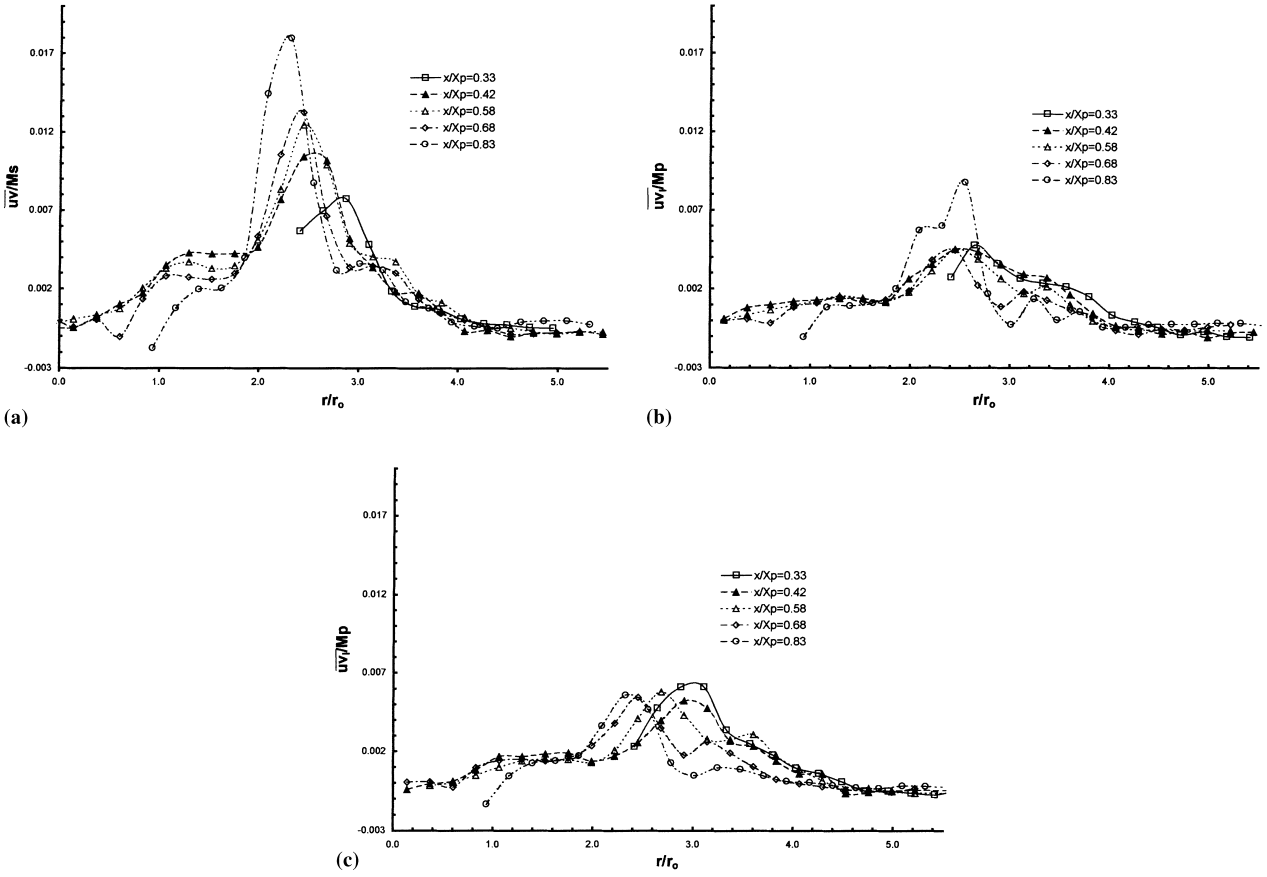

Fig. 9. (a) Intrinsic Reynolds shear stress for steady RJR flow: $V_0 = 48$ m/s, $b = 2.5$ mm, $X_p = 24$ mm. (b) Intrinsic Reynolds shear stress for pulsed RJR flow: $V_0 = 48$ m/s, $b = 2.5$ mm, $X_p = 24$ mm, 10 Hz pulsation frequency and $N = 1/3$. (c) Intrinsic Reynolds shear stress for pulsed RJR flow: $V_0 = 48$ m/s, $b = 2.5$ mm, $X_p = 24$ mm, 10 Hz pulsation frequency and $N = 2/3$.

understanding of the velocity field for pulsed flow prior to further modelling.

5. Velocity field investigation

5.1. Mean velocity field

The predicted velocity field is summarized in the vector plot of Fig. 4. The reattachment region is seen clearly. Use of measured mean axial and mean radial velocities, Bremhorst and Agnew (1996), leads to the qualitative flow representation of Fig. 5 which holds for both the steady and pulsed RJR flows, although for the latter it applies only in the later part of the cycle once the attached flow has been reestablished. From Fig. 5 it is seen that a secondary vortex exists which is absent in the predicted results of Fig. 4.

Corresponding pressure coefficients are given in Fig. 6 where a small radial shift between measured and predicted results is noted as well as a difference in the peak values. The predicted values in the centre region beneath the nozzle ($r/r_0 < 1$) are below the measured values thus indicating stronger suction than actually exists. This and the lower peak value at the reattachment point ($r/r_0 \approx 3.1$) indicate that the model does not yield the full recovery of pressure observed by measurement. The model is also unable to reproduce the low pressure peak within the stagnation region.

Comparing the radial and axial velocity fields for $N = 1/3$ and 2/3, shows little variation from the steady case, Bremhorst and Agnew (1996). In all cases, reattachment occurs near $r/r_0 = 3.1$ and a surface vortex is found together with a secondary recirculation region in the space between the nozzle and the surface. Only small variations with pulsing frequency were observed. The above results indicate little difference between the steady and pulsed RJR flows.

Extension of mean radial velocity measurements to the near wall region where the flow is essentially parallel to the wall, highlights a significant difference between the two types of flows, Fig. 7(a)–(c). The data were obtained in single channel mode in order to allow the measuring volume of the LDA to be brought almost to the solid surface. The radial measurement planes are located within the recirculation zone, near the stagnation or reattachment region and well outside of the recirculation region.

The limited data show a clear frequency dependency but more importantly, show that relative to the steady jet, wall damping of pulsations leads to a significant reduction in mean velocity parallel to the wall. A consequence of this is a reduction of mean velocity gradient at the wall which in turn will affect heat and mass transfer. This feature is a key indicator of why pulsed surface heat transfer Nusselt numbers for the range of pulsations studied, are not above those for the steady case.

5.2. Fluctuating velocity field – time means

Averaging over many pulses at a given point in the pulse, permits phase averaged means and phase averaged root mean squares of velocity fluctuations to be obtained. The latter can

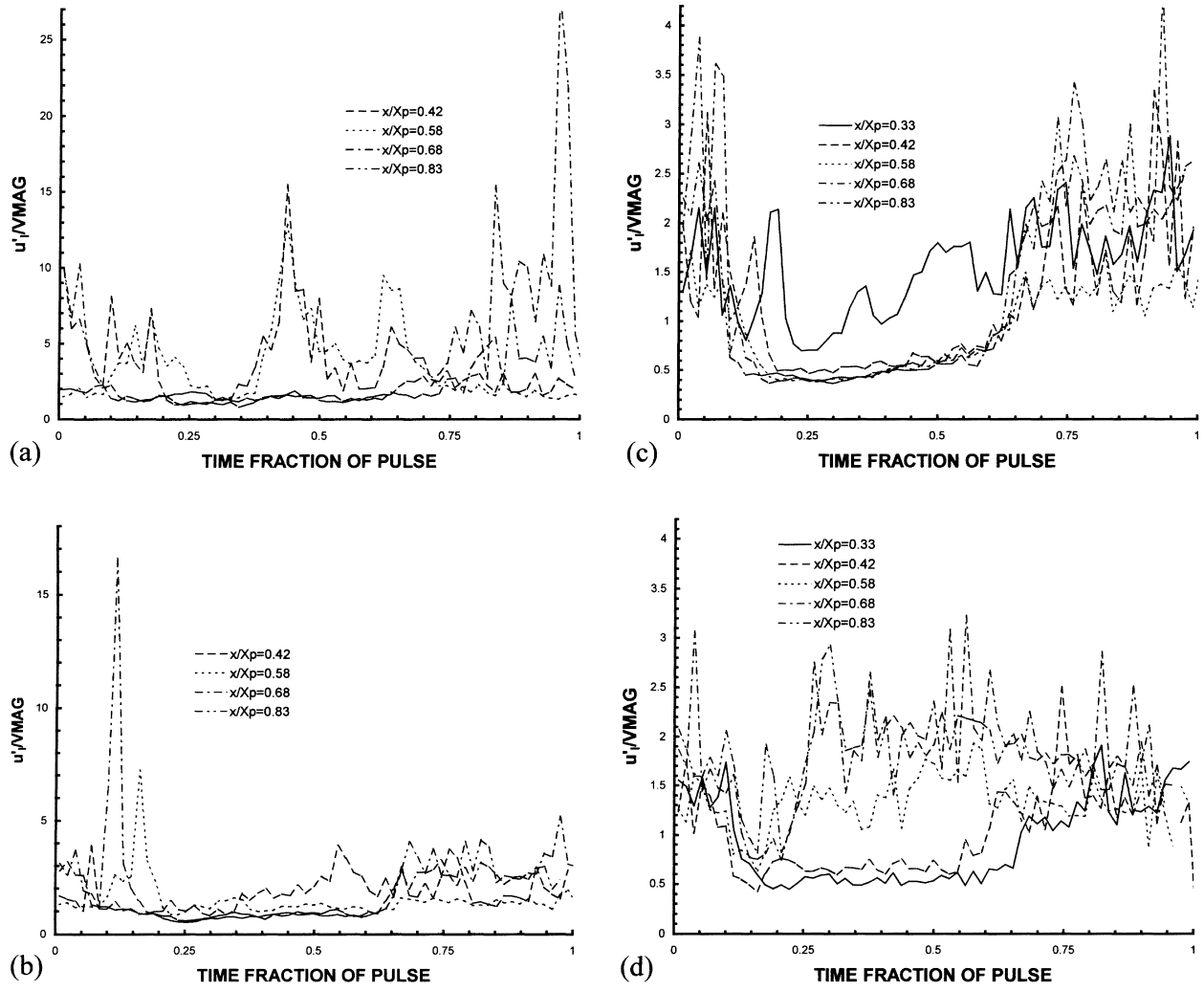

Fig. 10. Ensemble averaged axial intrinsic turbulence: $V_0 = 48$ m/s, $b = 2.5$ mm, $X_p = 24$ mm, 10 Hz and $N = 2/3$. (a) At nozzle radius, $r/r_0 = 1.0$. (b) Just inside reattachment region, $r/r_0 = 2.4$. (c) Near reattachment region, $r/r_0 = 3.1$. (d) In the wall jet region, $r/r_0 = 4.5$.

then be averaged over a cycle to give the average root mean square turbulence level at any point. This is the shear generated or intrinsic turbulence which is comparable to that of a steady flow. Fig. 8(a)–(c) show the case of steady and pulsed jet intrinsic turbulence levels. Considerable similarity is noted between the two cases both in distribution and in level. The similarity also applies to the radial component, Agnew (1996).

Transport by turbulence is through the Reynolds shear stresses. Fig. 9(a)–(c) show that unlike the normal stresses, these are different for steady and pulsed flow with the pulsed cases being significantly lower than for the steady one. Normalisation on jet exit momentum is used on the basis that jet momentum determines turbulent shear stresses as already found to be the case for pulsed free jets, Bremhorst and Hollis (1990). The reduced level of the shear stresses for the pulsed cases is further evidence of a reduction of transport by the small scale motions.

5.3. Fluctuating velocity field – phase averaged

From a modelling perspective, it is expected that quasi-steady state behavior results if the time scale of pulsation is large relative to the time scales of the turbulence. The flow behavior is then expected to be like a steady flow but with varying mass flow rate. On that basis, it is useful to consider flow variables as a function through the pulse, that is, phase averages. Agnew (1996) gives a comprehensive set of phase averaged turbulence quantities of which the most instructive are reproduced in Figs. 10–12. In order to facilitate comparison of measured turbulence levels with those of steady, free jets, components of root mean square intrinsic turbulence are normalized on the mean velocity magnitude, VMAG_τ, given by

$$\mathrm{VMAG}_\tau = \sqrt{(U_\tau^2 + V_\tau^2)}.$$

In order to keep data files of LDA signals within reasonable bounds, some scatter of phase averages has to be accepted. In spite of this, trends of the data are readily visible. Under the nozzle, the mean velocity at any instant through the pulse is very small, hence turbulence intensities are high. Prior to reattachment, a finite mean velocity exists during the "on" part of the cycle thus giving somewhat reduced turbulence intensity. A further reduction in mean velocity exists at the reattachment radius but near the wall at $x/X_p = 0.33$. This is near the stagnation point where a high turbulence level is observed. Much higher turbulence intensities exist during the deceleration and "off" part of the cycle when the periodic velocity is very small.

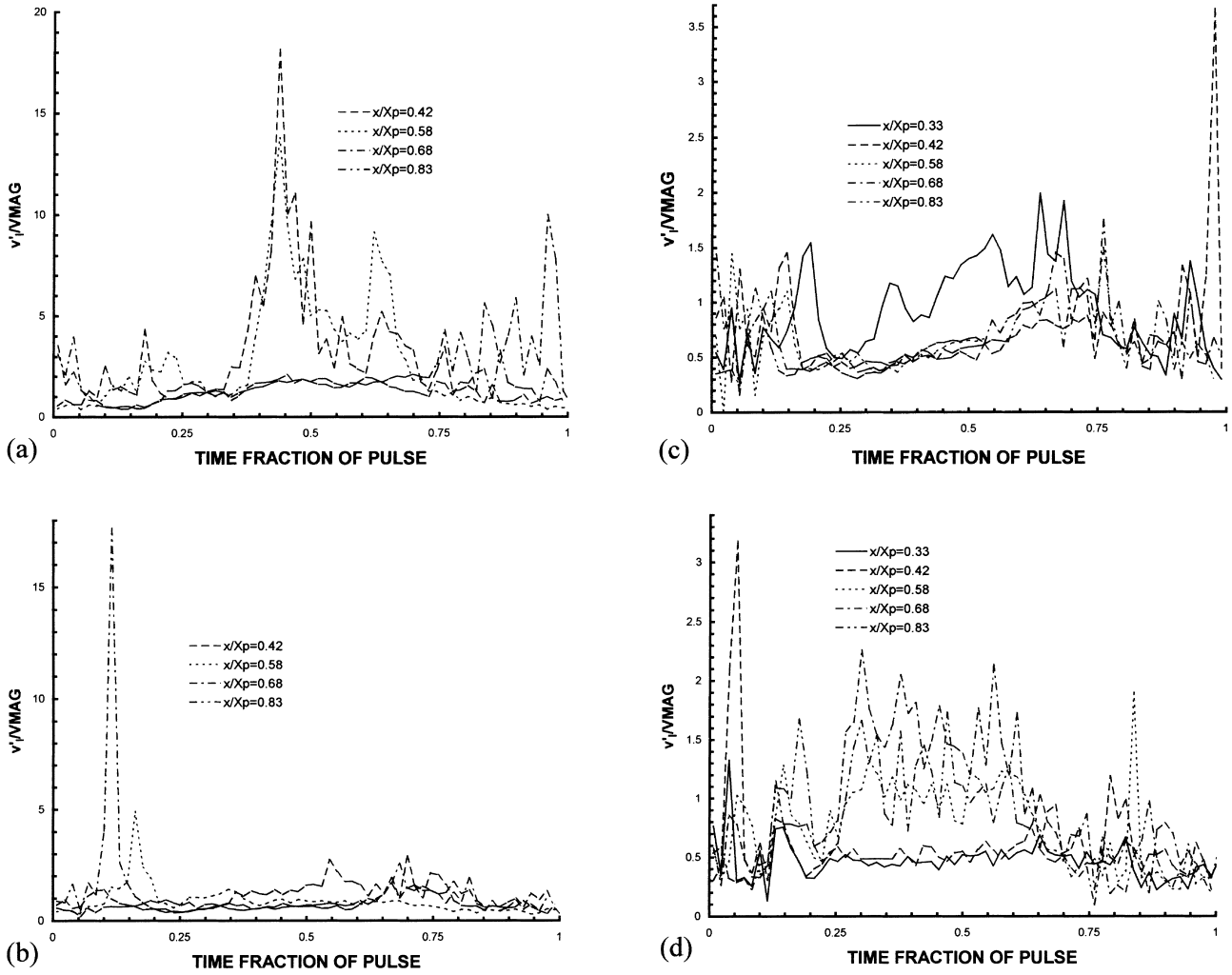

Fig. 11. Ensemble averaged radial intrinsic turbulence: $V_0 = 48$ m/s, $b = 2.5$ mm, $X_p = 24$ mm, 10 Hz and $N = 2/3$. (a) At nozzle radius, $r/r_0 = 1$. (b) Just inside reattachment region, $r/r_0 = 2.4$. (c) Near reattachment region, $r/r_0 = 3.1$. (d) In the wall jet region, $r/r_0 = 4.5$.

From Figs. 10 and 11 it is seen that for the on part of the cycle where turbulence intensities similar to those of free jets or in boundary layers can be expected if the flow is quasi-steady, the turbulence intensities and hence k, are much higher than for corresponding steady flows. This is consistent with findings in fully pulsed jets, Bremhorst and Hollis, 1990; Bremhorst et al., 1997, for which the intrinsic turbulence intensity is higher than that found in steady jets. The intrinsic covariances of Fig. 12 are particularly uncertain but the same trends seen above are still visible if the initial and final portions of a pulse are ignored as corresponding values for steady jets are typically 0.2 or less.

While qualitatively, the present flow would be expected to act like a quasi-steady one due to the very low Strouhal numbers (<0.005 based on exit slot width and exit velocity), the higher intrinsic turbulence level leads to modelling difficulties which still remain to be resolved even for the much simpler case of a fully pulsed, round jet, Graham and Bremhorst (1993).

6. Conclusions

Radial jet reattachment flow has associated with it a significantly higher surface heat transfer than in-line jets impinging normally to a surface. This has found use in the paper drying industry where even higher heat transfer rates are desired. Attempts to improve the surface heat transfer even further by periodic renewal of the trapped fluid in the recirculation zone under the nozzle, did not yield further improvements above those of the steady RJR flow although the heat transfer rates were a strong function of the length of the on period for the pulsed flow with a longer on period giving better heat transfer results.

Simple k-ϵ modelling of the flow with a turbulent Prandtl number to give surface heat transfer, led to reasonable predictions of surface heat transfer but results indicated that improvements in modelling are required.

Detailed velocity field measurements for the steady and fully pulsed RJR flow led to the realization that the pulsing effect does not penetrate the wall region fully thus leading to a reduced velocity gradient in the wall region and hence leading to a reduced temperature gradient.

Turbulence measurements indicated a lower relative turbulent shear stress which is consistent with the reduced heat transfer. Normal intrinsic turbulent stresses, even in regions where the flow more closely resembles free jet flow, were found to be higher for the pulsed jet than for the steady jet. This aspect was previously found to lead to

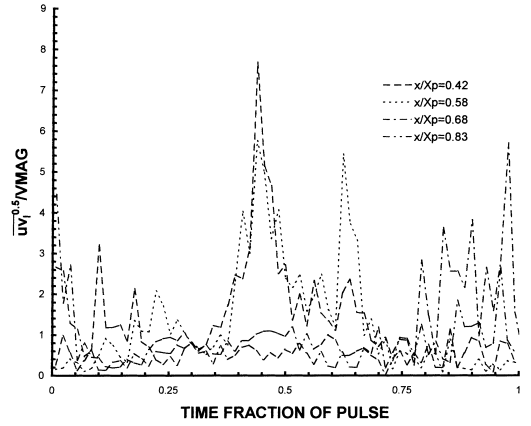

(a) At nozzle radius, r/r_o=1.0

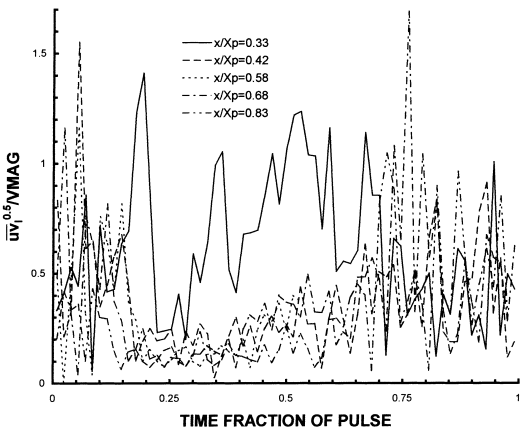

(c) Near reattachment region, r/r_o=3.1

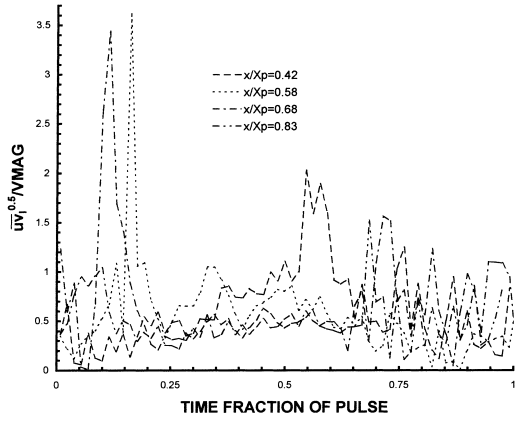

(b) Just inside reattachment region, r/r_o=2.4

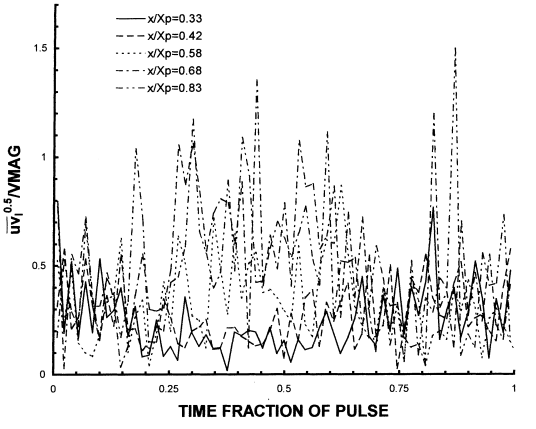

(d) In the wall jet region, r/r_o=4.5

Fig. 12. Ensemble averaged covariance of intrinsic turbulence: $V_0 = 48$ m/s, $b = 2.5$ mm, $X_p = 24$ mm, 10 Hz and $N = 2/3$. (a) At nozzle radius, $r/r_0 = 1.0$. (b) Just inside reattachment region, $r/r_0 = 2.4$. (c) Near reattachment region, $r/r_0 = 3.1$. (d) In the wall jet region, $r/r_0 = 4.5$.

significant flow modelling difficulties, Graham and Bremhorst (1993).

Acknowledgements

The authors wish to thank Professor R.H. Page, Texas A&M University, College Station, Texas for his generous assistance which made collection of the heat transfer data possible and Mr. T. Gruber, his student, for assistance with operation of the thermographic system.

Appendix A. Equations

For incompressible flow, invoking the Boussinesq relationship and the eddy viscosity relationship of

$$\nu_t = \frac{C_\mu k^2}{\varepsilon}.$$

Momentum:

$$U_j \frac{\partial U_i}{\partial x_j} = -\frac{1}{\rho}\frac{\partial P}{\partial x_i} + \frac{\partial}{\partial x_j}\left(\nu \frac{\partial U_i}{\partial x_j} - \overline{u_i u_j}\right).$$

Energy:

$$U_i \frac{\partial T}{\partial x_i} = \frac{\partial}{\partial x_i}\left[\left(\frac{\nu}{\mathrm{Pr}} + \frac{\nu_t}{\sigma_T}\right)\frac{\partial T}{\partial x_i}\right].$$

k-transport:

$$U_i \frac{\partial k}{\partial x_i} = \frac{\partial}{\partial x_i}\left[\frac{\nu_t}{\sigma_k}\frac{\partial k}{\partial x_i}\right] + \nu_t\left(\frac{\partial U_i}{\partial x_j} + \frac{\partial U_j}{\partial x_i}\right)\frac{\partial U_i}{\partial x_j} - \varepsilon.$$

ε-transport:

$$U_i \frac{\partial \varepsilon}{\partial x_i} = C_{1\varepsilon}\nu_t \frac{\varepsilon}{k}\left(\frac{\partial U_i}{\partial x_j} + \frac{\partial U_j}{\partial x_i}\right)\frac{\partial U_i}{\partial x_j} + \frac{\partial}{\partial x_i}\left(\frac{\nu_t}{\sigma_\varepsilon}\frac{\partial \varepsilon}{\partial x_i}\right) - C_{2\varepsilon}\frac{\varepsilon^2}{k}.$$

References

Agnew, N.D., 1991. An investigation of radial reattachment using laser Doppler anemometry and flow visualization, Undergraduate thesis, Department of Mechanical Engineering, The University of Queensland, St. Lucia, Brisbane, Australia.

Agnew, N.D., 1996. An investigation into fully pulsed radial jet reattachment, Ph.D. thesis, The University of Queensland, St. Lucia, Brisbane, Australia.

Bremhorst, K., Agnew, N.D., 1996. An investigation into the fully pulsed radial reattaching jet, FED-Vol. 237, 1996 Fluids Engineering Division Conference, ASME, vol. 2, pp. 589–594.

Bremhorst, K., Gehrke, P.J., He, S., Measured Reynolds stress distributions and energy budgets of fully pulsed round free jets and comparisons with k-ϵ model predictions, 11th Symposium on Turbulent Shear Flows, Institut, National Polytechnique, Universite Joseph Fourier, Grenoble, 8–10 September, 1997, vol. 22.1–22.6.

Bremhorst, K., Hollis, P.G., 1990. Velocity field of an axisymmetric pulsed, subsonic air jet. AIAA J. 28, 2043–2049.

Crowe, S.C., Champagne, F.H., 1971. Orderly structure in jet turbulence. Journal of Fluid Mechanics 84, 547–591.

Graham, L.J.W., Bremhorst, K., 1993. Application of the k–ε turbulence model to the simulation of a fully pulsed free air jet. Trans. ASME, J. Fluids Engrg. 115 (1), 70–74.

Hill, W.G. Jr., Greene, P.R., 1977. Increased turbulent jet mixing rates obtained by self-excited acoustic oscillation. Journal of Fluid Engineering, Trans. ASME, 99, 520–525.

Ostawari, C., Page, R.H., 1992. Convective heat transfer from a radial jet reattachment. AIChE Symposium Series, Heat Transfer, San Diego 88, 189–197.

Page, R.H., Kiel, R., 1990. Utilization of a radial jet reattachment for industrial drying. In: Proceedings of the Forum on Industrial Application of Fluid Mechanics, ASME FED, vol. 100, pp. 71–77.

Pepper, F., 1993. The self oscillating jet impingement nozzle, Studienarbeit, Texas A&M University, Department of Mechanical Engineering, College Station, Texas.

Winter, A., Graham, L.J.W., Bremhorst, K., 1991. Effects of velocity bias in LDA measurements using sample and hold processing. Experiments in Fluids 11, 147–152.